Gallium Arsenide Solar Cell Absorption Enhancement Using Whispering Gallery Modes of Dielectric Nanospheres

Jonathan Grandidier, *Member, IEEE*, Dennis M. Callahan, Jeremy N. Munday, *Member, IEEE*, and Harry A. Atwater

***Abstract*—Based on a perfectly flat gallium arsenide solar cell, we show that it is possible to modify the flow of light and enhance the absorption without modifying the active material structure or degrading its electrical properties. The sunlight couples into confined resonant modes formed by a periodic arrangement of dielectric nanospheres above the solar cell. The incoupling element is lossless and, thus, has the advantage that no energy is lost within the dielectric nanospheres. This stored energy is absorbed by the underlying active material which directly contributes to the photocurrent enhancement of the solar cell.**

***Index Terms*—Gallium arsenide, nanospheres, photovoltaic systems, whispering gallery modes (WGMs).**

I. Introduction

THE route to more than 30% single-junction solar cell efficiency requires the short-circuit current J_{SC}, the open-circuit voltage V_{OC}, and the fill factor to be near their theoretical maximum values. The current single-junction solar cell record at 1-sun illumination is 28.2% [1], which is for a GaAs cell. Investigating all optical methods to maximize J_{SC} without parasitic loss is of great importance, while reducing the thickness is needed to increase V_{OC}. Additionally, reducing the amount of material is necessary for reducing both the cost and weight of the cell, which requires advanced light-trapping strategies as the active layer is thinned [2].

Thin-film photovoltaics offer the possibility to significantly reduce the cost of a solar cell compared with first-generation solar cells, usually at the expense of efficiency. It is, therefore, of great interest to combine thin-film absorbing layers with advanced light-trapping schemes to reduce the cost without reducing the efficiency. Several light-trapping methods have already been proposed and demonstrated. Optimized antireflection coatings [3], Plasmonic gratings [4], [5], photonic crystals [6], [7], nano- and microwires [8], [9], nanodomes [10], and dielectric diffractive structures [11] are some of the light-trapping schemes that have been investigated. Ways to couple the light into guided modes [12] have also been studied and have shown significant increase in the optical path and in the absorption [13]. Light trapping is a critical requirement in thin-film photovoltaics, and dielectric texturing is a viable method to induce light trapping [14], but thin-film device quality often suffers upon direct texturing of the semiconductor active material. Texturing the active layer increases the path length of the incident photons and increases their probability to be absorbed, but it can be at the cost of limiting the solar cell's lifetime caused by faster cell degradations. It can also reduce the electrical properties of the solar cell by adding surface recombination. Thus, it is desirable to develop a simple, scalable design method in which textured dielectric layers provide for light trapping on smooth, planar thin-film cells. We propose here an approach for coupling light into smooth untextured thin-film solar cells [15] of uniform thickness using periodic arrangements of resonant dielectric nanospheres deposited as a continuous film on top of a thin cell. It is shown that guided whispering gallery modes (WGMs) in the spheres [16] can be coupled into particular modes of the solar cell and significantly enhance its efficiency by increasing the fraction of incident light absorbed [17]. We numerically demonstrate this enhancement using full-field finite-difference time-domain (FDTD) simulations of a silicon dioxide (SiO_2) nanosphere array above gallium arsenide (GaAs) solar cells featuring back reflectors and double antireflection coatings. The incoupling element in this design has advantages over other schemes as it is a lossless dielectric material, and its spherical symmetry naturally accepts a wide angle of incidence range. Moreover, analytical models show that for nanospheres of a given dielectric material, a large number of resonant modes can be supported, which can give rise to a 11% absorption enhancement in a 100-nm-thick GaAs absorber layer at several wavelengths between 300 and 900 nm and 2.5% enhancement in the case of a 1000-nm-thick GaAs absorber layer. In addition, the SiO_2 nanosphere array can be fabricated using simple, well-developed self-assembly methods and is easily scalable without the need for lithography or patterning. This concept can be easily extended to other thin-film solar cell materials, such as silicon or copper indium gallium diselenide.

WGM resonators have found numerous applications in science and technology due to their unique combination of small

Manuscript received July 7, 2011; revised November 23, 2011; accepted December 6, 2011. Date of publication January 13, 2012; date of current version March 16, 2012. The work of J. Grandidier and H. A. Atwater was supported by the Department of Energy "Light-Material Interactions in Energy Conversion" Energy Frontier Research Center under Grant DE-SC0001293. The work of D. M. Callahan and J. N. Munday was supported by the Office of Basic Energy Sciences under Contract DE-FG02-07ER46405.

J. Grandidier, D. M. Callahan, and J. N. Munday are with the Thomas J. Watson Laboratories of Applied Physics, California Institute of Technology, Pasadena, CA 91125 USA (e-mail: jgrandid@caltech.edu; callahan@caltech.edu; jnmunday@caltech.edu).

H. A. Atwater is with Thomas J. Watson Laboratories of Applied Physics and Kavli Nanoscience Institute California Institute of Technology, Pasadena, CA 91125, USA (e-mail: haa@caltech.edu).

Color versions of one or more of the figures in this paper are available online at http://ieeexplore.ieee.org.

Digital Object Identifier 10.1109/JPHOTOV.2011.2180512

size and high optical quality factors [18], [19]. We have demonstrated recently their use for solar applications in the case of a thin-film amorphous silicon solar cell [17]. GaAs is the semiconductor whose absorption is best matched with the solar spectrum [20] and which, currently, has the world record for single-junction solar cell efficiency at 1-sun illumination [1]. Moreover, it has already widely been investigated in several configurations [21]–[23]; therefore, we extend the concept of WGMs to a GaAs solar cell. We numerically demonstrate the optimal sphere size and spacing to achieve the highest possible photocurrent density for several thicknesses of GaAs solar cells with a double antireflection coating and a hexagonally close-packed array of silica spheres.

II. Modes of a Nanosphere

Solving the modes of a dielectric sphere in vacuum is a classic problem in electromagnetism [24], and it can be shown that a given sphere has several solutions that can be taken advantage of for solar cell enhancement. A dielectric sphere in vacuum can support *E*-type and *H*-type waves (for details, see [25]). For simplicity, we detail here only the calculation for *E*-type waves. For *E*-type waves, the admissible values of the parameter $k_0 a$ for a dielectric sphere are solutions of

$$\frac{\left[\sqrt{ka}J_\nu(ka)\right]'}{\sqrt{ka}J_\nu(ka)} = \left(\frac{\varepsilon}{\mu}\right)^{1/2} \frac{\left[\sqrt{k_0 a}H_\nu^{(1)}(k_0 a)\right]'}{\sqrt{k_0 a}H_\nu^{(1)}(k_0 a)} \quad (1)$$

where a is the radius of the sphere, k is the wave number, J_ν is the spherical Bessel function, and $H_\nu^{(1)}$ is the first kind spherical Hankel function. ε and μ are the dielectric constant and magnetic permeability of the sphere, and the prime means the derivative of the argument on which the function depends, here, ka or $k_0 a$. The electric field is described by

$$E(r,\theta,\varphi) \propto \vec{e}_r * n(n+1) P_n^m(\cos\theta) \frac{\sqrt{kr}Z_\nu(kr)}{(kr)^2} e^{\pm im\varphi} + \vec{e}_\theta * \frac{d}{d\theta}\left[P_n^m(\cos\theta)\right] \frac{1}{kr}\frac{d}{d(kr)}\left[\sqrt{kr}Z_\nu(kr)\right] e^{\pm im\varphi} \vec{e}_\varphi * \mathrm{i}\frac{\pm m}{\sin\theta} P_n^m(\cos\theta) \frac{1}{kr}\frac{d}{d(kr)}\left[\sqrt{kr}Z_\nu(kr)\right] e^{\pm im\varphi} \quad (2)$$

where P_n^m are the adjoint Legendre polynomials and $\vec{e}_r$, $\vec{e}_\theta$, $\vec{e}_\varphi$ are the unit vectors directed along the axes of the polar coordinate system fixed at the sphere surface. Z_ν corresponds to the Bessel function J_ν inside the sphere and the Hankel function $H_\nu^{(1)}$ of first kind outside the sphere. The boundary conditions impose continuity for the tangential components of the electric field. Fig. 1 shows the calculated field profiles of a cross section of a 700-nm silicon dioxide sphere of dielectric constant $\varepsilon = 1.462^2$ in a vacuum for several n and m mode orders. For each n values from $n = 1$ to $n = 3$, we represent the solution of (1), which corresponds to the highest wavelength. Most of the energy is present inside the dielectric sphere, and the field exponentially decays outside of the sphere. This corresponds to an evanescent wave described by the Hankel function shape of the mode. This behavior has some advantage for solar applications. Because most of the energy is stored inside the sphere, when it is above a higher index material, it will tend to naturally leak into it, which we show further for the case of a GaAs solar cell. Additionally, when two dielectric spheres are close enough, they have the ability to couple to each other [26]. When several sphere modes couple together due to their proximity, it can lead to waveguide formation [16]. Finally, when the spheres are hexagonally close packed, they can be excited by diffractive coupling and can all couple with each other [27].

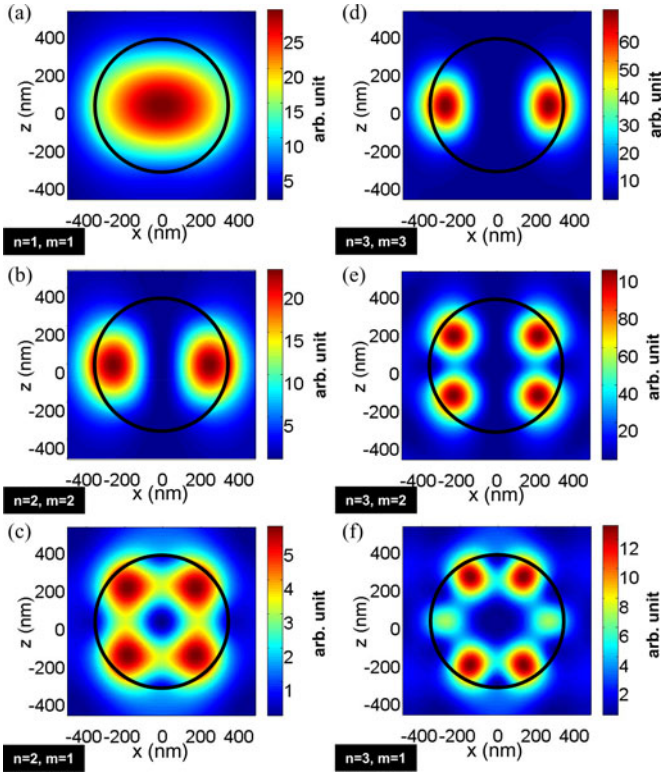

Fig. 1. Horizontal cross sections of the *E*-type eigenmode calculated with (2) corresponding to the highest wavelength, which is a solution of (1) for a 700-nm diameter silicon dioxide nanosphere in a vacuum. (a) $\lambda_1^h = 1147$ nm in the case $n = 1$ and $m = 1$. (b) and (c) $\lambda_2^h = 796$ nm in the case $n = 2$ and, respectively, $m = 2$ and $m = 1$. (d)–(f) $\lambda_3^h = 602$ nm in the case $n = 3$ and, respectively, $m = 3$, $m = 2$, and $m = 1$. The black circles show the contour of the sphere.

III. Flat Gallium Arsenide Solar Cell

We first consider a GaAs solar cell with a 40-nm-thick titanium dioxide (TiO_2) and 90-nm-thick SiO_2 double-layer antireflection coating and a silver back reflector. A broadband wave pulse with the electric field polarized along the *x*-axis is injected at normal incidence on the structure, and the fields are monitored at 300 wavelengths equally spaced between $\lambda = 300$ nm and $\lambda = 900$ nm. This wavelength range corresponds to the sun's energy spectrum below the bandgap of GaAs. The optical generation rate in the GaAs is calculated using [28]

$$G_{\mathrm{opt}}^n(\omega) = \int \frac{\varepsilon''(\omega)|E(\omega)|^2_{\mathrm{GaAs}}}{2\hbar}\Gamma_{\mathrm{solar}}(\omega)dV \quad (3)$$

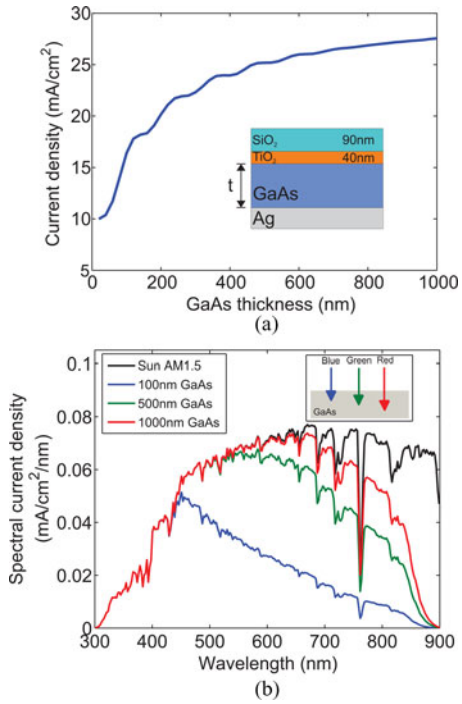

Fig. 2. (a) Current density of a flat GaAs solar cell with back reflector and double antireflection coating as a function of the GaAs thickness. (b) Calculated spectral current density for different GaAs layer thicknesses. The spectral range is weighted by the solar spectrum and compared with the AM1.5 solar spectrum.

where $|E(\omega)|^2_{\mathrm{GaAs}}$ is the electric field intensity integrated over the GaAs volume [29] and $\varepsilon''(\omega)$ is the imaginary part of the dielectric function of the GaAs. $\Gamma_{\mathrm{solar}}(\omega)$ is a factor used to weight each wavelength by the AM1.5 solar spectrum. We represent in Fig. 2(a) the current density of a flat GaAs solar cell with back reflector and double antireflection coating as a function of the GaAs thickness. The current density considerably increases within the first 500 nm. This shows that most of the light is absorbed within this range. For a 500-nm-thick GaAs solar cell, we calculate a current density of 25.19 mA/cm^2. Then, above 500 nm, the current density slowly increases to reach 27.56 mA/cm^2 for a 1000-nm-thick GaAs solar cell. This value corresponds to 82% of the maximum attainable value. Even though this value is high, it still gives potential for improvement.

We present in Fig. 2(b) the AM1.5 solar spectrum and plots that indicate the fraction of the solar energy absorbed in three thin GaAs layers on a single pass. The current density is calculated by $J = G^n_{\mathrm{ana}}(\omega) * q$ where q is the electron charge and

$$G^n_{\mathrm{ana}}(\omega) = \alpha(\omega) N_0 \int e^{-\alpha(\omega)x} dx \tag{4}$$

is the analytically calculated optical generation rate. N_0 is the sun photon flux at the top of the GaAs layer and $\alpha(\omega) = 4\pi\sqrt{\varepsilon''(\omega)}/\lambda$ is the absorption coefficient. Fig. 2(b) gives us an indication of where in the spectral range there exists potential for improvement to increase the absorption in a GaAs absorbing layer for the three considered thicknesses. Clearly, a large fraction of the solar spectrum is poorly absorbed, especially in the 600–900 nm spectral range for the case of a 1000-nm-thick

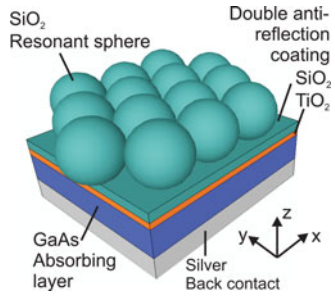

Fig. 3. Schematic of a GaAs solar cell with hexagonally close-packed SiO_2 nanospheres on top of it.

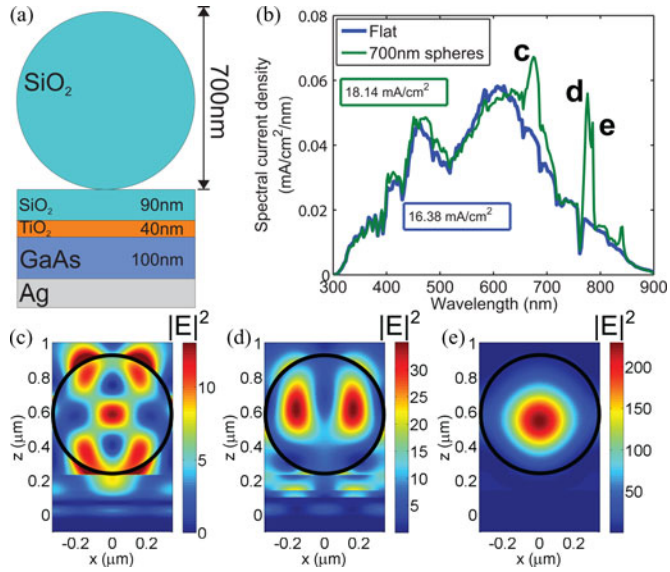

Fig. 4. (a) Cross section of a silica nanosphere on a flat GaAs solar cell with back reflector and double-layer antireflection coating. (b) Spectral current density of a 100-nm-thick GaAs flat cell and a cell with a hexagonally close-packed monolayer array of 700-nm diameter dielectric nanospheres. Each peak labeled (c), (d), and (e) correspond to different WGM orders where we show the electric field intensity for a cross section at the middle of a sphere at different wavelengths for the labeled peaks. The E field of the initial plane wave is oriented in the xz plane. The black circles show the contour of the sphere.

GaAs absorbing layer. Thus, a way to increase the absorption in this particular wavelength range will have a direct influence on the solar cell's efficiency. We develop in the next section a way to significantly increase the light absorption in the weakly absorbing part of a GaAs solar cell by using the WGMs of a dielectric nanosphere monolayer array.

IV. Nanospheres Atop a Gallium Arsenide Solar Cell

In order to estimate the influence of a hexagonally close-packed monolayer array of dielectric nanospheres atop the flat GaAs solar cell (see Fig. 3), we perform 3-D FDTD electromagnetic simulations to determine the expected absorption enhancement. A schematic of the cross section is represented in Fig. 4(a). In Fig. 4(b), we compare the expected spectral current density in the case of a flat GaAs solar cell and a cell with a hexagonally close-packed monolayer array of 700-nm dielectric nanospheres for a 100-nm-thick GaAs solar cell. The dip between 450- and 600-nm wavelengths is due to Fabry–Pérot

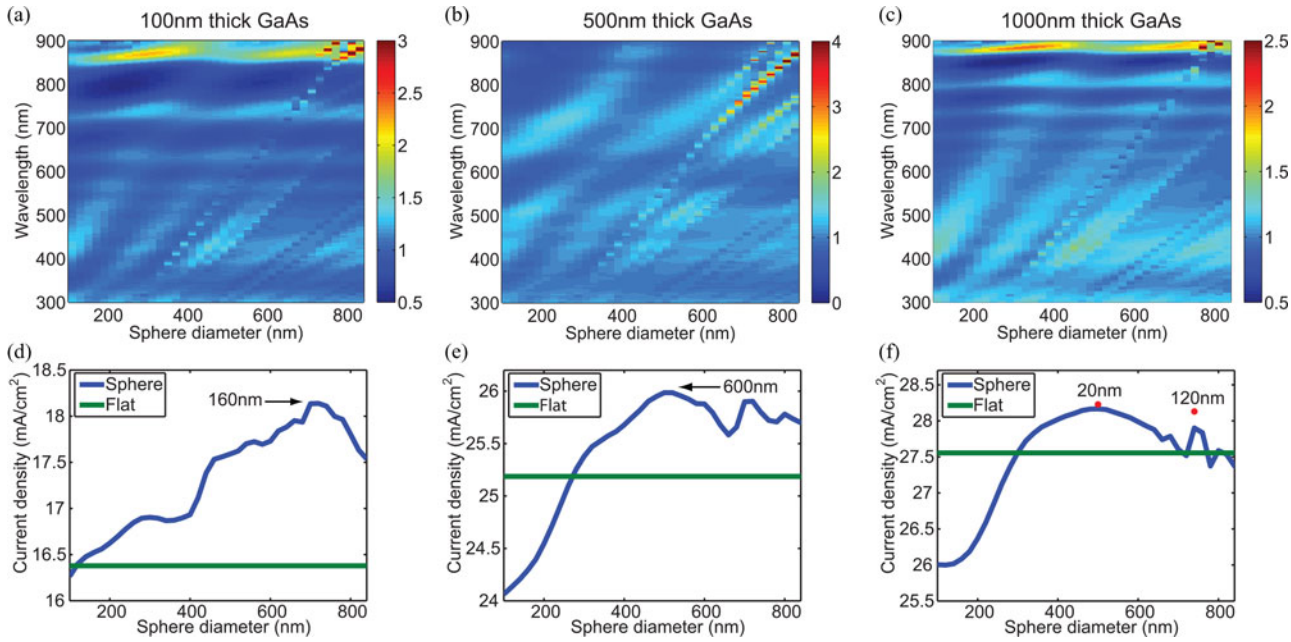

Fig. 5. Ratio between the spectral current density of a solar cell with hexagonally close-packed spheres over the spectral current density of a solar cell without spheres for a (a) 100-nm, (b) 500-nm, and (c) 1000-nm-thick GaAs solar cell. (d)–(f) Current density of a solar cell as a function of the sphere diameter above it. The current of the equivalent flat cell is also represented. (d) and (e) represent the highest value obtained with sphere what thickness of an equivalent flat GaAs solar cell would be. In (f), the red dots show the value for the written spacing between the spheres.

interference in the flat region of the solar cell. The dip appears in an off-resonance range where the influence of the spheres is negligible, evidenced by the same dip's occurrence in the flat configuration. We labeled several peaks corresponding to different WGM orders in the nanospheres [30] above the solar cell. For the case represented in Fig. 4(d), the enhancement due to the sphere's WGM is more than 300%. Because, in the near infrared part of the solar spectrum, GaAs is weakly absorbing, we are able in this case, due to the monolayer spheres array, to enhance the generated current density by more than 11%. Interestingly, the mode profiles that we see in Fig. 4(c)–(e) are very similar to the ones we analytically calculated and represented in Fig. 1. This gives us a clear demonstration of the relation between the excitation of WGMs and the current density enhancement at the wavelength at which it occurs.

In Fig. 5(a)–(c), we illustrate the ratio between the spectral current density of a solar cell with hexagonally close-packed spheres over the spectral current density of a solar cell without spheres for three different thicknesses of GaAs: 100, 500, and 1000 nm, respectively. The spheres' diameter varies between $D = 100$ nm and $D = 900$ nm. Strong enhancement occurs corresponding to optical dispersion of the array of coupled WGM dielectric spheres. In Fig. 5(d)–(f), we plot the current density as a function of the sphere diameter for the same GaAs thicknesses previously described. In the case of the 100-nm-thick GaAs solar cell, the highest current density is obtained for 700-nm diameter spheres and equals $J = 18.14$ mA/cm^2 [see Fig. 5(d)]. In the case of a flat GaAs solar cell, the same current density would be obtained for a 160-nm-thick GaAs solar cell, which means that in this particular case, it is possible to save 37.5% of the active material to obtain the same amount of current density. In Fig 5(a), the enhancement due to the WGMs clearly appears in the range between 700- and 900-nm wavelengths where the enhancement lines directly refer to the WGM orders. In the case of the 500-nm-thick GaAs solar cell, the highest current density is obtained with 500-nm diameter hexagonally close-packed nanospheres on top of it and equals $J = 26.00$ mA/cm^2. This corresponds to a 3.2% enhancement compared with a flat GaAs solar cell with double antireflection coating where the current density equals $J = 25.19$ mA/cm^2. Note that, as shown in Fig. 2(a), in order to obtain the same current density with a flat GaAs solar cell, we would have need 600 nm of active material. For the case of the 1000-nm-thick GaAs solar cell, the highest current is obtained for $D = 500$ nm diameter spheres and is equal to $J = 27.41$ mA/cm^2 [see Fig. 5(f)]. Some enhancement for subwavelength diameter spheres is also seen, probably due to scattering effects [11]. There is still room for improvement for each of these cell thicknesses as the currents are not yet at the maximum attainable value, even for the 1000-nm-thick cell. The current densities can potentially be increased further by utilizing spheres of multiple diameters, partially embedding the spheres or texturing the underlying AR coatings. For a given peak resonance, the absorption is also influenced by the distance between the sphere array and the GaAs layer. Therefore, there exists an optimal distance between the sphere array and the absorbing layer, which can be tuned to maximize the absorption related to each independent peak due to the WGMs. However, modifying the distance between the spheres and the absorbing layer affects the effective double-layer antireflection coating thickness and can potentially degrade the performance of the cell off WGM resonances. The influence of the distance between the sphere array and the absorbing layer utilizing a model based on the

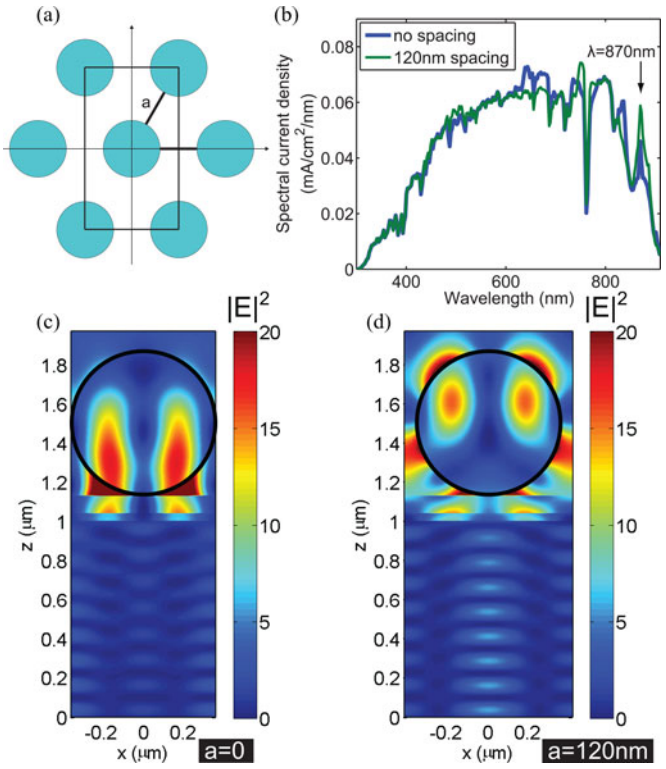

Fig. 6. (a) Top view of the periodic arrangement of the nanospheres with a spacing between them. The rectangle indicates the unit cell used for numerical simulations. (b) Comparison of the spectral current density of a 1000-nm-thick GaAs flat cell in the case where 740-nm nanospheres are hexagonally close packed and in the case where there is an $a = 120$ nm gap between them. (c), (d) Corresponding field profile at the resonant wavelength $\lambda = 870$ nm. The black circles show the contour of the sphere.

coupled mode theory is currently under investigation and will be discussed elsewhere. If we slightly tune the spacing between the spheres to $a = 20$ nm, it reaches $J = 28.23$ mA/cm^2, which corresponds to an enhancement of 2.5% compared with a flat solar cell with double antireflection coating. As we can see in Fig. 4, the enhancement occurs mainly at wavelength scale diameter spheres where low-order WGMs occur. In the case of 740-nm-diameter nanospheres, we can show that by tuning the spacing to $a = 120$ nm between the spheres, we can increase the spectral current from $J = 27.90$ mA/cm^2 for a hexagonally close-packed array of nanospheres to $J = 28.13$ mA/cm^2. This represents an enhancement of 2% compared with a flat solar cell with double antireflection coating. While this enhancement is less than shown earlier for the case of the 500-nm-diameter sphere array with 20-nm spacing, a part of the enhancement occurs near the band edge, which may be beneficial for thin cells. This improvement due to the spacing is detailed in Fig. 6. At $\lambda = 870$ nm, there exists a WGM effect that can be significantly enhanced with the spacing between the nanospheres as can be seen on Fig. 6(b). In order to understand this enhancement, we plot, in Fig. 6(c), the field profile of a cross section at the middle of a sphere in the xz plane at $\lambda = 870$ nm for a hexagonally close-packed array of nanospheres and compare it with the case where the spheres are $a = 120$ nm away from each other. It appears that this separation results in a greater coupling between the array of spheres and the active material. This is most likely due to a better coupling between the spheres themselves, as the field profile suggests.

V. Conclusion

We demonstrated light absorption enhancement on a 100-nm, a 500-nm, and a 1000-nm-thick GaAs solar cell structure featuring a back reflector, a double-layer antireflection coating, and a close-packed silica nanosphere array. The thinner the cell, the more the potential for improvement. We could see the highest improvement of 11% for the 100-nm GaAs solar cell by adding 700-nm hexagonally close-packed SiO_2 nanospheres on top of it. We could see that depending on the size of the spheres, the enhancement we obtain occurs on different parts of the spectrum. Therefore, the best current densities are obtained where WGMs enhance the weakly absorbing region of the active material. By optimizing the sphere size and spacing, we showed an improvement of 2.5% in the current generation for the case of a 1000-nm-thick GaAs solar cell. We also showed that the overall absorption enhancement obtained with thinner absorbing layers, around 100 nm, is much greater. In the case of a 1000-nm-thick GaAs solar cell, because the initial absorption is very high for the considered flat structure, the improvement using a single size nanosphere structure is much less; however, there is still improvement potential in the range 800–900 nm, leading to total absorbed currents close to the maximum attainable value.

Acknowledgment

The authors would like to thank I. S. Grudinin from the Jet Propulsion Laboratory for useful discussions.

References

[1] B. M. Kayes, presented at the 37th IEEE Photovoltaic Spec. Conf., Seattle, WA, 2011.
[2] H. A. Atwater and A. Polman, "Plasmonics for improved photovoltaic devices," *Nature Mater.*, vol. 9, pp. 205–213, 2010.
[3] J. Zhao and M. A. Green, "Optimized antireflection coatings for high-efficiency silicon solar cells," *IEEE Trans. Electron Devices*, vol. 38, no. 8, pp. 1925–1934, Aug. 1991.
[4] R. A. Pala, J. White, E. Barnard, J. Liu, and M. L. Brongersma, "Design of plasmonic thin-film solar cells with broadband absorption enhancements," *Adv. Mater.*, vol. 21, pp. 3504–3509, 2009.
[5] J. N. Munday and H. A. Atwater, "Large integrated absorption enhancement in plasmonic solar cells by combining metallic gratings and antireflection coatings," *Nano Lett.*, vol. 11, no. 6, pp. 2195–2201, 2011.
[6] J. D. Joannopoulos, P. R. Villeneuve and S. Fan, "Photonic crystals: Putting a new twist on light," *Nature*, vol. 386, pp. 143–149, 1997.
[7] P. Bermel, C. Luo, L. Zeng, L. C. Kimerling, and J. D. Joannopoulos, "Improving thin-film crystalline silicon solar cell efficiencies with photonic crystals," *Opt. Exp.*, vol. 15, pp. 16 986–17 000, 2007.
[8] M. D. Kelzenberg, S. W. Boettcher, J. A. Petykiewicz, D. B. Turner-Evans, M. C. Putnam, E. L. Warren, J. M. Spurgeon, R. M. Briggs, and N. S. Lewis, "Enhanced absorption and carrier collection in Si wire arrays for photovoltaic applications," *Nature Mater.*, vol. 9, pp. 239–244, 2010.
[9] E. Garnett and P. Yang, "Light trapping in silicon nanowire solar cells," *Nano Lett.*, vol. 10, pp. 1082–1087, 2010.
[10] J. Zhu, C.-M. Hsu, Z. Yu, S. Fan, and Y. Cui, "Nanodome solar cells with efficient light management and self-cleaning," *Nano Lett.*, vol. 10, pp. 1979–1984, 2010.
[11] M. Kroll, S. Fahr, C. Helgert, C. Rockstuhl, F. Lederer, and T. Pertsch, "Employing dielectric diffractive structures in solar cells—A numerical study," *Physica Status Solidi (a)*, vol. 205, pp. 2777–2795, 2008.

[12] J. Grandidier, S. Massenot, G. Colas des Francs, A. Bouhelier, J.-C. Weeber, L. Markey, A. Dereux, J. Renger, M. U. González, and R. Quidant, "Dielectric-loaded surface plasmon polariton waveguides: Figures of merit and mode characterization by image and Fourier plane leakage microscopy," *Phys. Rev. B*, vol. 78, p. 245419, 2008.
[13] P. N. Saeta, V. E. Ferry, D. Pacifici, J. N. Munday, and H. A. Atwater, "How much can guided modes enhance absorption in thin solar cells?," *Opt. Exp.*, vol. 17, pp. 20975–20990, 2009.
[14] E. Yablonovitch and G. D. Cody, "Intensity enhancement in textured optical sheets for solar cells," *IEEE Trans. Electron Devices*, vol. ED-29, no. 2, pp. 300–305, Feb. 1982.
[15] Z. Yu, A. Raman, and S. Fan, "Fundamental limit of nanophotonic light trapping in solar cells," in *Proc. Nat. Acad. Sci. USA*, 2010, vol. 107, pp. 17491–17496.
[16] A. Yariv, Y. Xu, R. K. Lee, and A. Scherer, "Coupled-resonator optical waveguide: A proposal and analysis," *Opt. Lett.*, vol. 24, pp. 711–713, 1999.
[17] J. Grandidier, D. M. Callahan, J. N. Munday, and H. A. Atwater, "Light absorption enhancement in thin-film solar cells using whispering gallery modes in dielectric nanospheres," *Adv. Mater.*, vol. 23, pp. 1272–1276, 2011.
[18] V. B. Braginsky and V. S. Ilchenko, "Properties of optical dielectric microresonator," *Sov. Phys. Dokl.*, vol. 32, pp. 306–307, 1987.
[19] V. S. Ilchenko and A. B. Matsko, "Optical resonators with whispering-gallery modes—Part II: Applications," *IEEE J. Sel. Topics Quantum Electron.*, vol. 12, no. 1, pp. 15–32, Jan./Feb. 2006.
[20] C. H. Henry, "Limiting efficiencies of ideal single and multiple energy gap terrestrial solar cells," *J. Appl. Phys.*, vol. 51, pp. 4494–4500, 1980.
[21] C. Colombo, M. Heiβ, M. Grätzel, and A. Fontcuberta i Morral, "Gallium arsenide p-i-n radial structures for photovoltaic applications," *Appl. Phys. Lett.*, vol. 94, pp. 173108-1–173108-3, 2009.
[22] K. Nakayama, K. Tanabe, and H. A. Atwater, "Plasmonic nanoparticle enhanced light absorption in GaAs solar cells," *Appl. Phys. Lett.*, vol. 93, pp. 121904-1–121904-3, 2008.
[23] B. M. Kayes, H. A. Atwater, and N. S. Lewis, "Comparison of the device physics principles of planar and radial p-n junction nanorod solar cells," *J. Appl. Phys.*, vol. 97, pp. 114302-1–114302-11, 2005.
[24] J. A. Stratton, *Electromagnetic Theory*. New York: McGraw-Hill, 1997.
[25] A. N. Oraevsky, "Whispering-gallery waves," *Quantum Electron.*, vol. 32, pp. 377–400, 2002.
[26] K. Hayata, H. Yénaka, and M. Koshiba, "Theory of coherent optical coupling between dielectric microspheres," *Opt. Lett.*, vol. 18, pp. 1385–1387, 1993.
[27] X. Yu, L. Shi, D. Han, J. Zi, and P. V. Braun, "High quality factor metallodielectric hybrid plasmonic–photonic crystals," *Adv. Funct. Mater.*, vol. 20, pp. 1910–1916, 2010.
[28] V. E. Ferry, J. N. Munday, and H. A. Atwater, "Design considerations for plasmonic photovoltaics," *Adv. Mater.*, vol. 22, pp. 4794–4808, 2010.
[29] A. D. Yaghjian, "Internal energy, Q-energy, Poynting's theorem, and the stress dyadic in dispersive material," *IEEE Trans. Antennas Propag.*, vol. 55, no. 6, pp. 1495–1505, Jun. 2007.
[30] R. M. Cole, Y. Sugawara, J. J. Baumberg, S. Mahajan, M. Abdelsalam, and P. N. Bartlett, "Easily coupled whispering gallery plasmons in dielectric nanospheres embedded in gold films," *Phys. Rev. Lett.*, vol. 97, pp. 137401-1–137401-4, 2006.

Jonathan Grandidier (M'11) received the Ph.D. degree in physics from the University of Burgundy, Dijon, France, in 2009.

He is currently a Postdoctoral Research Scholar of applied physics with the California Institute of Technology, Pasadena. His research interest is focused on new concepts for photovoltaics based on resonant dielectric structures. Prior to this, his work was centered on dielectric-loaded surface plasmon polariton waveguides for telecommunications. His work has been presented at international conferences and published in different international journals, and he has contributed chapters to one book.

Dr. Grandidier is a member of the International Society for Optics and Photonics and the Materials Research Society. He received a fellowship from Carnot Foundation, where he has been a member since 2009.

Dennis M. Callahan received the S.B. degree in chemical engineering from Northeastern University, Boston, MA, in 2008. He is currently working toward the Ph.D. degree in materials science with the California Institute of Technology, Pasadena.

His current research interests include design and fabrication of new types of solar cells in which the electromagnetic environment has been intentionally engineered to enhance performance, in particular, solar cells in which the local density of optical states is not homogeneous. His research interests also include solar cells incorporating elements of plasmonics, photonic crystals, optical resonators, and other areas of nanophotonics.

Jeremy N. Munday (M'06) received the B.S. degree in physics and astronomy from Middle Tennessee State University, Murfreesboro, in 2003 and the M.A. and Ph.D. degrees in physics from Harvard University, Cambridge, MA, in 2005 and 2008, respectively.

He is currently an Assistant Professor with the Department of Electrical and Computer Engineering and the Institute for Research in Electronics and Applied Physics, University of Maryland, College Park. Prior to this appointment, he was a Postdoctoral Research Scholar with the California Institute of Technology, Pasadena. His research has focused on next-generation photovoltaics, alternative energy, engineering acoustic and electromagnetic materials, plasmonics, and quantum electrodynamic phenomena, such as the Casimir effect. His research has been published in a variety of international journals, and he has contributed chapters to two books.

Dr. Munday is a member of the American Physical Society, Sigma Pi Sigma, the Materials Research Society, and the International Society for Optics and Photonics. He is a recipient of National Science Foundation fellowship.

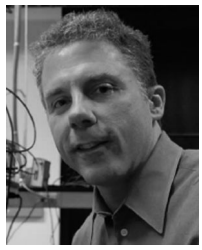

Harry A. Atwater received the S.B., S.M., and Ph.D. degrees in electrical engineering from the Massachusetts Institute of Technology, Cambridge, in 1981, 1983, and 1987, respectively.

He is currently a Howard Hughes Professor and Professor of applied physics and materials science with the California Institute of Technology, Pasadena. His research interests focus on two interwoven research themes: photovoltaics and solar energy and plasmonics and optical metamaterials. He has been active in photovoltaics research for more than 20 years. Recently, he has pioneered a new photovoltaic device, i.e., the silicon wire array solar cell, and has developed new fabrication approaches to III–V semiconductor multijunction cells, as well as making advances in plasmonic light absorber structures for III–V compounds and silicon thin films.